

## ARTICLE

# Penetration of linezolid and tedizolid in cerebrospinal fluid of mouse and impact of blood–brain barrier disruption

Marin Lahouati<sup>1,2</sup> | Mélanie Oudart<sup>1,2</sup> | Philippe Alzieu<sup>2</sup> | Candice Chapouly<sup>2</sup> | Antoine Petitcollin<sup>3</sup> | Fabien Xuereb<sup>1,2</sup> 

<sup>1</sup>Service de Pharmacie Clinique, CHU de Bordeaux, Hôpital Pellegrin, Bordeaux, France

<sup>2</sup>INSERM U1034, Biologie des Maladies Cardiovasculaires, Université de Bordeaux, Pessac, France

<sup>3</sup>Laboratoire de Pharmaco-Toxicologie Biologique et Médico-Légale, CH Tarbes-Lourdes, Tarbes, France

## Correspondence

Marin Lahouati, Service de Pharmacie, Hôpital Pellegrin, Centre Hospitalo-Universitaire de Bordeaux, Place Amélie Raba Léon, Bordeaux, 33000, France.  
Email: [marin.lahouati@chu-bordeaux.fr](mailto:marin.lahouati@chu-bordeaux.fr)

## Abstract

Penetration of antimicrobial treatments into the cerebrospinal fluid is essential to successfully treat infections of the central nervous system. This penetration is hindered by different barriers, including the blood–brain barrier, which is the most impermeable. However, inflammation may lead to structural alterations of these barriers, modifying their permeability. The impact of blood–brain barrier disruption on linezolid and tedizolid (antibiotics that may be alternatives to treat nosocomial meningitis) penetration in cerebrospinal fluid (CSF) remains unknown. The aim of this study is to evaluate the impact of blood brain barrier disruption on CSF penetration of linezolid and tedizolid. Female C57BI/6J mice were used. Blood–brain barrier disruption was induced by an intraperitoneal administration of lipopolysaccharide. Linezolid (40 mg/kg) or tedizolid-phosphate (20 mg/kg) were injected intraperitoneally. All the plasma and CSF samples were analyzed with a validated UPLC-MS/MS method. Pharmacokinetic parameters were calculated using a non-compartmental approach based on the free drug concentration. The penetration ratio from the plasma into the CSF was calculated by the AUC<sub>0-8h</sub> (Area Under Curve) ratio (AUC<sub>0-8hCSF</sub>/AUC<sub>0-8hplasma</sub>). Linezolid penetration ratio was 46.5% in control group and 46.1% in lipopolysaccharide group. Concerning tedizolid, penetration ratio was 5.5% in control group and 15.5% in lipopolysaccharide group. In conclusion, CSF penetration of linezolid is not impacted by blood–brain barrier disruption, unlike tedizolid, whose penetration ratio increased.

## Study Highlights

### WHAT IS THE CURRENT KNOWLEDGE ON THE TOPIC?

Blood–brain barrier disruption has an impact on cerebrospinal fluid penetration of drugs. Available literature data suggest a favorable cerebrospinal fluid-to-plasma concentration ratio for linezolid in infected human, however, a high interindividual variability is observed. On the opposite, there are few data concerning penetration of tedizolid in cerebrospinal fluid (CSF). Mechanisms of

CSF penetration and role of blood–brain barrier disruption of these drugs remain unknown.

#### WHAT QUESTION DID THIS STUDY ADDRESS?

What is the role of blood–brain barrier disruption on cerebrospinal fluid penetration of linezolid and tedizolid?

#### WHAT DOES THIS STUDY ADD TO OUR KNOWLEDGE?

Cerebrospinal fluid penetration of linezolid is not impacted by blood–brain barrier disruption, unlike tedizolid, whose cerebrospinal fluid penetration ratio increased from 5.5% to 15.5% in conditions of blood–brain barrier disruption.

#### HOW MIGHT THIS CHANGE CLINICAL PHARMACOLOGY OR TRANSLATIONAL SCIENCE?

We developed a mouse model to explore the pharmacokinetics of drugs' penetration in the cerebrospinal fluid under conditions of blood–brain barrier disruption. Tedizolid appears to be a potential candidate for treating staphylococcal-associated CNS infections.

## INTRODUCTION

Penetration of antimicrobial treatments into the cerebrospinal fluid (CSF) is essential to successfully treat infections of the central nervous system (CNS).<sup>1</sup> This penetration is hindered by different barriers, including the blood–brain barrier (BBB), which is the most impermeable.<sup>2</sup> The BBB is located on cerebral capillaries and comprises continuous endothelial cells with tight and adherent junctions, ensuring barrier impermeability and CNS protection.<sup>2</sup> Consequently, treatment of CNS diseases relies on the effective penetration of the active substance across the BBB. Various intrinsic molecular parameters influence the drugs diffusion across the BBB, such as molecular size, electric charge, lipophilicity, plasma protein binding and affinity for transport systems.<sup>3</sup> However, extrinsic factors can also influence CNS penetration of drugs such as architectural disruption of the BBB. Inflammation observed during a CNS infection like meningitis may lead to structural alterations of the BBB increasing permeability, and thus increasing penetration of some drugs in the CNS.<sup>1,4</sup> This effect is exploited in the treatment of meningitis by vancomycin: inflammatory response induced by the infection enhances vancomycin penetration into CSF from 14% to 48%.<sup>1</sup> Vancomycin is recommended as first-line treatment of nosocomial meningitis by the Infectious Diseases Society of America (IDSA).<sup>5</sup> Linezolid (LNZ), an oxazolidinone antibiotic, is recommended as an alternative to vancomycin by the IDSA to treat nosocomial CNS infections.<sup>5</sup> It acts as an inhibitor of protein synthesis by binding to the 23S rRNA component of the 50S subunit of the bacterial ribosome.<sup>6</sup> Literature data suggest a favorable CSF-to-plasma concentrations ratio

for LNZ in infected human with an area under the curve (AUC) CSF/Plasma ratio from 70% to 90%.<sup>3,7</sup> However, some studies suggest a high variability of CSF penetration in human<sup>8</sup> and the mechanism of LNZ diffusion across the BBB remains unknown. Tedizolid (TDZ) is also an oxazolidinone, but it remains active on linezolid-resistant bacterial strains,<sup>9</sup> and has a favorable safety profile, according to a recent study.<sup>10</sup> However, discrepant data are published concerning CSF penetration of TDZ.<sup>11,12</sup> Moreover, to our knowledge, there is no data about the impact of BBB disruption on CSF penetration of TDZ. Thus, the aim of this study is to evaluate the impact of BBB disruption induced by inflammation on CSF penetration of LNZ and TDZ in mice.

## MATERIALS AND METHODS

### Animals

Female C57BI/6J mice aged 12-week were used. Euthanasia was performed by exsanguination under deep anesthesia (ketamine 100 mg/kg and xylazine 20 mg/kg, intraperitoneally) or by cervical dislocation.

### Chemicals and reagents

LNZ (CAS 165800-03-3, purity 98%) and TDZ-phosphate (CAS 856867-55-5 purity 98%) were provided by ThermoFisher®. Both LNZ and TDZ-phosphate were dissolved by dimethyl sulfoxide (10%), polyethylene glycol 300 (40%), polysorbate 80 (5%), and sodium chloride (NaCl) 0.9% (45%). Linezolid, tedizolid, powders

intended for the confection of reagents for antibiotics assay in blood and CSF of mice were purchased from Alsachim®.

## BBB disruption

BBB disruption was induced by IP administration of lipopolysaccharide (LPS). LPS was derived from *Escherichia coli* O111:B4 (Sigma L2630) and was dissolved in 0.9% NaCl. A single dose of LPS at 10 mg/kg was administered to mice intraperitoneally. BBB disruption was assessed using immunoglobulin G (IgG) extravasation into the brain. BBB disruption was not evaluated more than 8.5 h after LPS administration due to poor tolerance of LPS.

## CSF and blood sampling

Analgesia was obtained by subcutaneous injection of buprenorphine (0.05 mg/kg) 30 min before sampling. Mice were anesthetized with isoflurane (3% for induction and 1% for maintenance) (Virbac Schweiz®, Glattbrugg, Germany) during blood and CSF sampling. For CSF sampling, the neck skin was incised, and muscles were dissected to expose the cisterna magna. CSF samples were collected from the region 5 of the cerebellum/spinal cord using stereotaxis and a 1.3 mm glass capillary. CSF was diluted in 0.9% NaCl (1:10) and stored at  $-80^{\circ}\text{C}$  in Eppendorf® tubes.

Retro-orbital route was used for blood sampling. Blood (500  $\mu\text{L}$ ) was transferred into Eppendorf® tubes containing ethylene diamine tetra acetic acid (EDTA) as anticoagulant (1:10 v:v EDTA:blood). Plasma was separated by an 8-min centrifugation at 12,000g and then stored at  $-80^{\circ}\text{C}$  in Eppendorf® tubes.

## Brain tissue sampling

A flushing of the vessels was performed through intracardiac perfusion with a 0.9% NaCl solution. The brain was then removed by a sagittal sectioning between the hemispheres.

## Immunohistochemistry

Collected brains were fixed in 10% formalin for 4 h, incubated in 30% sucrose overnight and embedded in optimal cutting temperature. Subsequently, 9-micron-thick

sections were cut (cryomicrotome Leica CM3050S®). Anti-podocalyxin antibodies (R&D Systems® reference AF1556) were used at 1:200 v:v to identify brain vessels (endothelial cells). They were resolved using Alexa® fluor-conjugated secondary polyclonal antibodies (green) at 1:400 v:v (ThermoFisher reference 10246392). Anti-IgG antibodies conjugated with a fluorochrome of a different color (red) were added to assess their diffusion through the vessels (1:400 v:v, ThermoFisher® reference 10236683). Images were captured with Axiozoom® V16 microscope (Zeiss) under 260 $\times$  magnification. Three pictures were acquired per animal. A random number was assigned to each image and analysis was performed in a blinded model.

## Concentration measurement in plasma

For antibiotics extraction from plasma samples or quality controls (QC), 10  $\mu\text{L}$  of a methanol/water (50:50 v:v) solution and 30  $\mu\text{L}$  of an acetonitrile/methanol (95:5 v:v) precipitating solution containing the internal standards at 1.00  $\mu\text{g/mL}$  were added to 10  $\mu\text{L}$  of thawed plasma or QC. For the extraction of the standards, blank human plasma was used instead of sample or QC, and the blank methanol/water solution was replaced by a methanol/water (50:50 v:v) solution containing the desired concentration of LNZ and TDZ. The calibration curve comprised 10 calibration standard points (0.00; 0.10; 0.25; 0.50; 1.00; 2.50; 5.00; 10.00; 25.00; 50.00  $\mu\text{g/mL}$ ). After centrifugation for 10 min at 18,000g, the supernatant was diluted (1:10 v:v) in water and transferred in a glass vial before injection of 3  $\mu\text{L}$  into the chromatographic system.

## Concentration measurement in CSF

A similar procedure was used for the extraction of CSF samples, with the exception that blank plasma was replaced by artificial blank CSF prepared by dilution (1:10 v:v) with phosphate buffer saline (PBS) (pH=7.4) containing 2% (m/V) of bovin serum albumin (BSA) with 0.9% NaCl. The internal standards in the precipitating solution were set at a concentration of 100 ng/mL. Furthermore, after centrifugation, the supernatant was not diluted and was transferred directly in a glass vial before injection of 3  $\mu\text{L}$  into the chromatographic system. Also, the calibration curve was adapted to the concentrations in CSF, and was prepared with 11 points (0.0; 1.0; 2.5; 5.0; 10.0; 25.0; 50.0; 100.0; 500.0; 1000.0; 2500.0 ng/mL).

## UPLC-MS/MS conditions

Total LNZ and TDZ concentrations in plasma and CSF samples were analyzed using ultra high-performance liquid chromatography/tandem mass spectrometry (UPLC-MS/MS). Chromatographic separation was achieved on an Acquity® H-Class UPLC (Waters®) with a C18 BEH® (1.7  $\mu$ m, 2.1  $\times$  50 mm column) thermostated at 40°C. The flow rate was 0.5 mL/min with a binary gradient using mobile phase A (0.02% ammonia and 0.1% formic acid in water) and mobile phase B (0.1% formic acid in acetonitrile). The gradient was as follows: 97% A (0–0.5 min), 97% to 30% A (0.5–2.0 min), 0% A (2.1–3.0 min), and back to 97% A (3.1–4.0 min). The total run duration was 4 min.

The detection was performed on a TQ-XS® (Waters®) tandem mass spectrometer operating in multiple reaction monitoring (MRM) mode. The following MRM transitions were monitored: LNZ: 338.1 > 296.2 (quantifier) and 338.1 > 195.2 (qualifier); TDZ: 371.0 > 343.0 (quantifier) and 371.0 > 288.0 (qualifier); [2H8]-LNZ 346.1 > 304.2 (internal standard); [13C,2H3]-TDZ 375.0 > 347.0 (internal standard).

## Method validation

Analytical methods were validated according to the European Medicine Agency guideline on bioanalytical method validation, including the evaluation of accuracy, precision, stability, dilution integrity, matrix effect, selectivity, and carryover.<sup>13</sup> The methods intended for CSF and plasma were validated independently from each other. Dilution integrity up to 1:20 v:v was verified for both methods, and there was no significant matrix effect, nor carryover or selectivity issues. The main parameters describing the analytical performances of the method are given in [Appendix 1](#).

## Pharmacokinetic study

The pharmacokinetic parameters of single-dose LNZ or TDZ were evaluated. A single dose of LNZ at 40 mg/kg or TDZ-phosphate at 20 mg/kg was administered by intraperitoneal (IP) route. For each molecule, 30 mice were randomly assigned to control group ( $n=15$ ) or to LPS group ( $n=15$ ). In LPS groups, a single dose of LPS (10 mg/kg) was administered intraperitoneally 30 min before injection of LNZ or TDZ-phosphate. Mice were sampled 30 min, 1 h, 2 h, 4 h, and 8 h after LNZ administration (3 mice at each timepoint), and 30 min, 1 h, 4 h, 6 h, and 8 h after TDZ-phosphate administration (3 mice at each timepoint).

Pharmacokinetic parameters (elimination constant ( $K_e$ ), elimination half-life ( $t_{1/2}$ ), maximum concentration ( $C_{max}$ ), time to reach  $C_{max}$  ( $T_{max}$ ), clearance and area under the concentration–time curve from 0 to 8 h ( $AUC_{0-8h}$ ) were calculated using a non-compartmental model using PK Solver software (version 2.0). The penetration ratio of the drug from the plasma into the CSF was calculated by the  $AUC_{0-8h}$  ratio ( $AUC_{0-8hCSF}/AUC_{0-8hplasma}$ ). Pharmacokinetic plasma parameters were evaluated based on the free drug concentration calculated with protein binding of 31% for LNZ<sup>14</sup> and 74.8% for TDZ.<sup>15</sup>

## Ethics statement

All animal experiments were carried out in accordance with the guidelines of European Parliament Directive 2010/63/EU on the protection of animals used for scientific purposes and were approved by the local Animal Care and Use Committee of Bordeaux University (CE050), under protocol number DAP37876-V2-2022092910487439. The animals were housed in a conventional animal facility and were monitored daily for appearance, weight, clinical signs, and behavior to prevent animal pain and minimize distress.

## RESULTS

### BBB disruption

BBB is disrupted at each timepoint after LPS administration ([Figure 1a,b](#)). The ratio of the mean areas of IgG in the inflammatory condition/mean areas of IgG in the control condition at each timepoint after administration of LPS shows that the BBB is disrupted between 60 and 510 min, and that the opening is greater from 270 min post-LPS administration.

## Pharmacokinetic study

### Linezolid

Mean  $C_{max}$  in the control group was 27,781 ng/mL (SD: 7049 ng/mL) in plasma and 13,147 ng/mL (SD: 2125 ng/mL) in CSF. In LPS group,  $C_{max}$  (plasma) was 26,751 ng/mL (SD: 5095.9 ng/mL) and  $C_{max}$  (CSF) 14,477 ng/mL (SD: 3998.1 ng/mL).  $AUC_{0-8h}$  penetration ratio was 46.5% in the control group and 46.1% in the LPS group. In the LPS group, LNZ concentrations in plasma and CSF are more sustained over time from 2 h after injection of LNZ

and  $T_{1/2}$  elimination is almost doubled in the LPS group. Pharmacokinetics parameters of LNZ in both conditions are reported in Table 1 and Figure 2.

## Tedizolid

Mean  $C_{\max}$  in control group was 2761 ng/mL (SD: 461.7 ng/mL) in plasma and 187.9 ng/mL (SD: 142 ng/mL) in CSF. In the LPS group,  $C_{\max}$  (plasma) was 2926.35 ng/mL (SD: 694 ng/mL) and  $C_{\max}$  (CSF) 755.4 ng/mL (SD: 546 ng/mL).  $AUC_{0-8h}$  penetration ratio was 5.5% in control group and 15.5% in LPS group. The profiles of the concentration curves for TDZ in plasma appear to be comparable, although the profiles of the curves in CSF differ between the two groups, with the AUC for TDZ in the LPS group being three times higher.

Pharmacokinetics parameters in both conditions are reported in Table 2 and Figure 3.

## DISCUSSION

Inflammation caused by CNS infections, such as meningitis, led to increased BBB permeability influencing antimicrobial penetration in CNS.<sup>1</sup> Studying the CNS penetration of antibiotics in these inflammatory conditions is important for proposing adapted drugs to treat patients. To date, we have successfully developed a mouse model to study drug penetration into the CSF under conditions of BBB disruption. In vitro or in silico models may also be used to understand drug penetration into CSF<sup>16</sup> however for severe infections, characterized by significant structural and molecular dysfunction,<sup>4</sup> in vivo models are necessary to

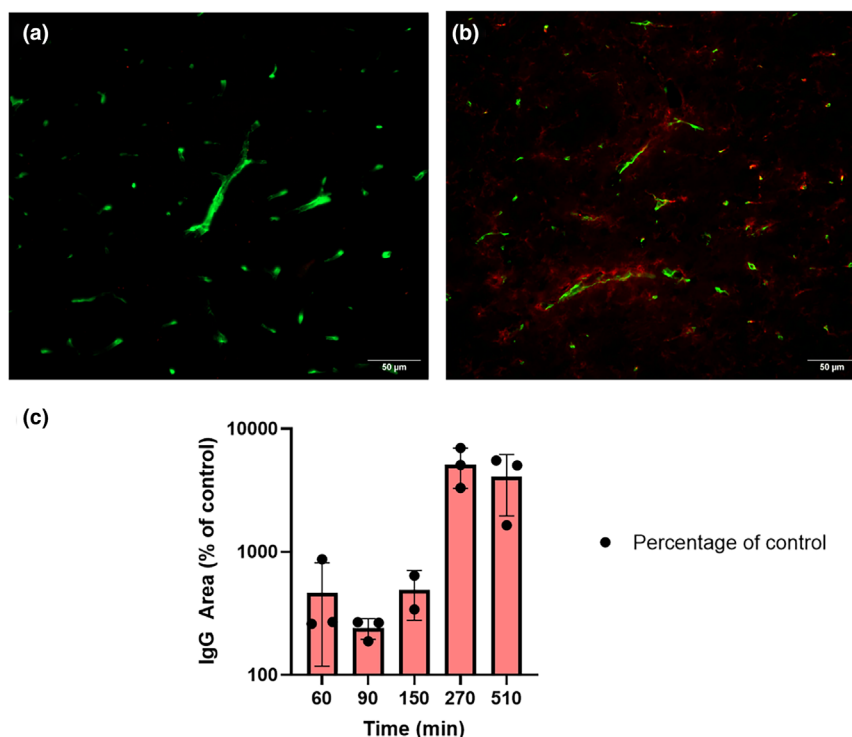


**FIGURE 1** Blood–brain barrier disruption after LPS administration. (a) control and (b) LPS show IgG (red) penetration through vessels (green) in brain of mice. (c) is the ratio of the mean areas of IgG LPS/LPS-free conditions (3 mice for each time and condition).

**TABLE 1** Pharmacokinetic parameters of linezolid.

| Parameters         | Unit    | LNZ <i>n</i> = 15 |          | LNZ + LPS <i>n</i> = 15 |          |
|--------------------|---------|-------------------|----------|-------------------------|----------|
|                    |         | Plasma            | CSF      | Plasma                  | CSF      |
| $T_{1/2}$          | h       | 2                 | 1.8      | 3.8                     | 2.9      |
| $T_{\max}$         | h       | 1                 | 1        | 0.5                     | 0.5      |
| $C_{\max}$ (mean)  | ng/mL   | 27,781            | 13,147.5 | 26,751.3                | 14,477.5 |
| Clearance          | mL/h    | 1                 | 2,2      | 0.47                    | 1.14     |
| $AUC_{0-8h}$       | ng/mL*h | 82,938.6          | 38,580.2 | 149,982.4               | 69,145.9 |
| Ratio $AUC_{0-8h}$ | –       | 46.5%             |          | 46.1%                   |          |

Abbreviations: AUC, area under the concentration–time curve;  $C_{\max}$ , maximum concentration; CSF, cerebrospinal fluid; LNZ, linezolid; LPS, lipopolysaccharide;  $T_{1/2}$ , elimination half-life;  $T_{\max}$ , time to reach  $C_{\max}$ .



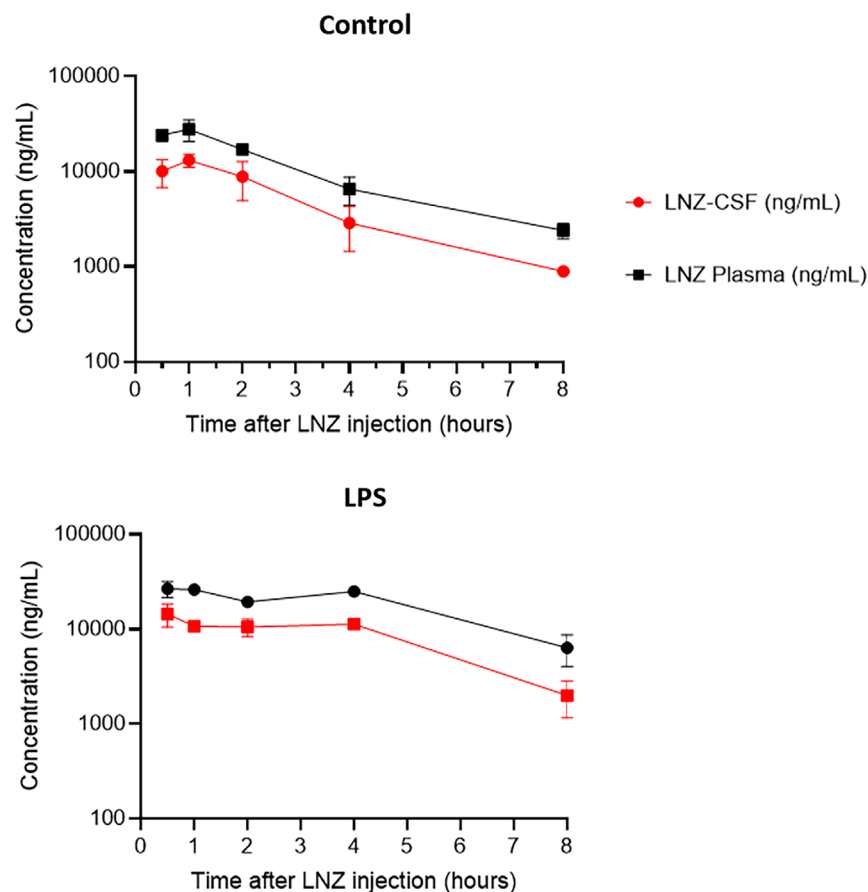


**FIGURE 2** Plasma and CSF concentration–time profiles of linezolid in mouse received a single dose (40 mg/kg) of linezolid (upper section) and a single dose (40 mg/kg) of linezolid combined with LPS injection (10 mg/kg) 30 min before linezolid administration (lower section).

| Parameters                | Unit    | TDZ (n = 15) |                   | TDZ + LPS (n = 15) |        |
|---------------------------|---------|--------------|-------------------|--------------------|--------|
|                           |         | Plasma       | CSF               | Plasma             | CSF    |
| $T_{1/2}$                 | h       | 5.3          | 4.8 <sup>a</sup>  | 20.8               | 6.8    |
| $T_{max}$                 | h       | 4            | 0.5               | 1                  | 0.5    |
| $C_{max}$                 | ng/mL   | 2761.1       | 187.9             | 2926.3             | 755.4  |
| Clearance                 | mL/h    | 1.39         | 17.6 <sup>a</sup> | 0.45               | 6.3    |
| AUC <sub>0-8h</sub>       | ng/mL*h | 18,431.1     | 1005.4            | 19,917.5           | 3092.3 |
| Ratio AUC <sub>0-8h</sub> | –       | 5.5%         |                   | 15.5%              |        |

**TABLE 2** Pharmacokinetic parameters of tedizolid.

Abbreviations: AUC, area under the concentration–time curve;  $C_{max}$ , maximum concentration; CSF, cerebrospinal fluid; LPS, lipopolysaccharide;  $T_{1/2}$ , elimination half-life; TDZ, tedizolid;  $T_{max}$ , time to reach  $C_{max}$ .

<sup>a</sup>CSF  $T_{1/2}$  evaluated with 24 h pharmacokinetic (Appendix 2).

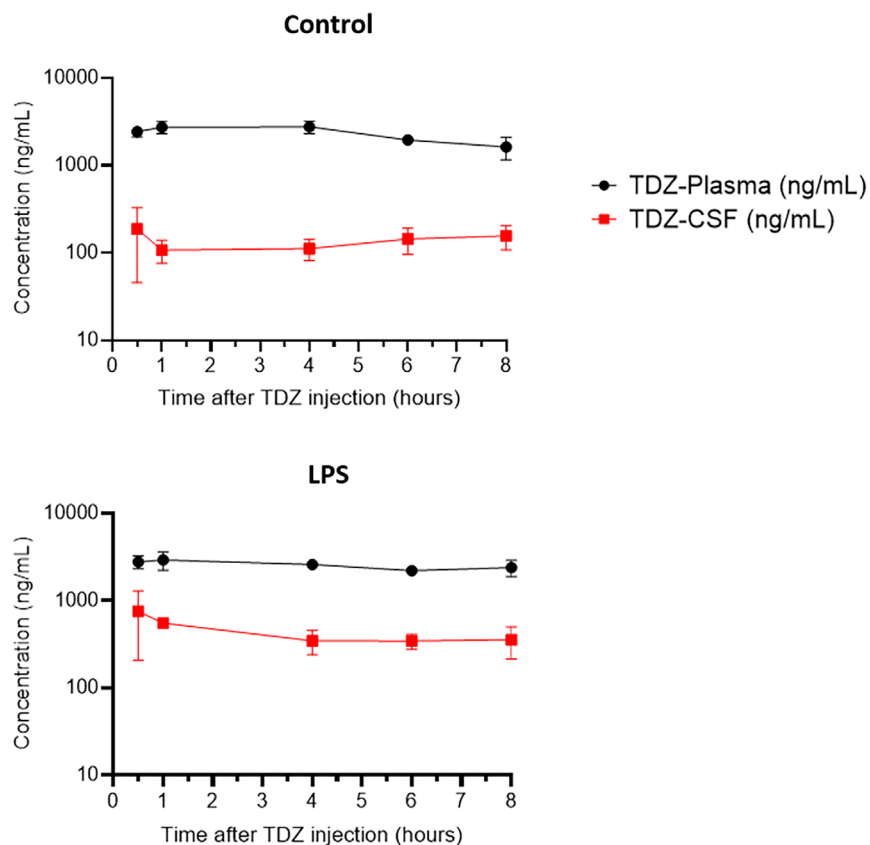
explore drug penetration under these circumstances. Mice offer several advantages over other mammals, notably high repeatability at a lower cost. Moreover, the BBB architecture of mice closely resembles that of humans, allowing us to better understand the mechanisms of drug penetration into the CSF.<sup>17</sup> At last, LPS induced systemic inflammation similar to infection,<sup>4,18</sup> thus mimicking the pharmacokinetic changes observed during this condition.<sup>19</sup>

We highlighted that BBB disruption has no impact on the CSF penetration of LNZ. Thus, BBB disruption does not appear to be responsible for interindividual

variations of CSF penetration observed in humans. CSF penetration of drugs is also mediated by influx or efflux pumps such as P-gp, BCRP, or OAT.<sup>20</sup> To date, it is not known if LNZ is a substrate of one or several of these pumps. However, this could be an explanation for the observed interindividual and inter-species variations, as these pumps are not expressed at the same levels across species.<sup>20</sup> Other studies using in vitro and in vivo models of BBB and pharmacological inhibitors such as these pumps may help to identify which of them is implicated in CSF penetration of LNZ.

**FIGURE 3** Plasma and CSF

concentration–time profiles of tedizolid in mouse received a single dose (20 mg/kg) of tedizolid (upper section) and a single dose (20 mg/kg) of tedizolid combined with LPS injection (10 mg/kg) 30 min before tedizolid administration (lower section).



Regarding TDZ, we found that the penetration ratio increases in the condition of BBB disruption (from 5.5% to 15.5%). There are few studies reporting TDZ penetration in CSF: Gu et al. reported a CSF penetration of 2.16% in a non-inflammatory model of rat,<sup>12</sup> however, they evaluated the AUC penetration ratio using total concentration, without taking into account the protein binding coefficient of TDZ. Wenzler et al.<sup>11</sup> reported a CSF penetration ratio of about 50% (free drug concentration ratio) in a patient treated with TDZ for an *Enterococcus faecium* meningitis. This ratio is higher than the one in our study; however, it may be explained by inter-species variability between humans and mice.<sup>21</sup>

The PK/PD index of TDZ that best correlates with efficacy is the ratio of the area under the free drug concentration–time curve at steady state over 24 h to the minimal inhibitory concentration (MIC) ( $fAUC_{24h}/MIC$ ) over 3.<sup>22</sup> In our study, for a MIC of 0.5  $\mu\text{g/mL}$  which is the EUCAST/CA-SFM cutoff sensitivity for *Staphylococcus aureus*,<sup>23</sup>  $fAUC(CSF)_{24h}/MIC$  is 4 in healthy condition. It was not possible to calculate  $fAUC_{24h}(CSF)/MIC$  in the condition of BBB disruption, because of the poor tolerability of LPS. However, an increase of TDZ penetration in CSF led to  $fAUC_{8h}/MIC$  of 6.2 in the LPS group, whereas it was only 2 in healthy conditions suggesting that PK/PD index  $fAUC_{24h}(CSF)/MIC$  should be greater in BBB disruption condition. However, while our findings suggest

an increased PK/PD index for TDZ under conditions of BBB disruption, caution must be taken when extrapolating  $AUC_{8h}$  to  $AUC_{24h}$ , as CSF clearance may not precisely mirror plasma clearance over time particularly because of variation in permeability of BBB. Further studies in humans are needed to confirm these results, but TDZ appears to be a potential candidate for treating staphylococcal-associated CNS infections.

This study has several limitations. First, despite a similar BBB architecture between mice and humans, variation in protein expression, such as efflux pumps may limit the extrapolation of CSF penetration ratios between species.<sup>21</sup> However, these results may help to understand the CSF penetration of oxazolidinone. Then, we used a high dose of LPS to disrupt the BBB. This high dose was not well tolerated by mice, and it was not possible to perform a 24-h pharmacokinetic study. Moreover, LPS induced changes in pharmacokinetic parameters, decreasing drug clearance and increasing absorption speed, which led to an increase in  $AUC_{8h}$ , especially for LNZ due to its short elimination half-life. In the future, it would be interesting to compare these results with experiments using lower repeated doses of LPS in an attempt to limit its systemic effects on pharmacokinetic parameters. Additionally, models of chronic BBB disruption and neuroinflammation may be used, such as experimental autoimmune encephalomyelitis<sup>24</sup> or

hyperammonemia<sup>25</sup> to compare the CSF penetration of drugs between models. Lastly, we chose to use a single-dose administration for LNZ, and thus, we cannot draw conclusions on PK/PD objectives due to the short elimination half-life of LNZ.

In conclusion, we developed a mouse model to explore the pharmacokinetics of oxazolidinones in the CSF under conditions of BBB disruption. CSF penetration of LNZ is not impacted by BBB disruption, unlike TDZ, whose CSF penetration ratio increased from 5.5% to 15.5% in conditions of BBB disruption. This model may be a useful tool to explore new drugs' CSF penetration during pre-clinical studies.

## AUTHOR CONTRIBUTIONS

M.L., M.O. and A.P. wrote the manuscript; M.L., C.C. and F.X. designed the research; M.L., M.O., P.A. and A.P. performed the research; M.L. and F.X. analyzed the data.

## ACKNOWLEDGMENTS

We would like to thank the entire U1034 laboratory team, especially Marie-Ange Renault, Alain-Pierre Gadeau and Thierry Couffignal for their valuable discussions and feedback. We also thank Sylvain Grolleau and Maxime David for their technical assistance.

## FUNDING INFORMATION

No funding was received for this work.

## CONFLICT OF INTEREST STATEMENT

The authors declared no competing interests for this work.

## ORCID

Fabien Xuereb  <https://orcid.org/0000-0002-2240-196X>

## REFERENCES

- Nau R, Sörgel F, Eiffert H. Penetration of drugs through the blood-cerebrospinal fluid/blood-brain barrier for treatment of central nervous system infections. *Clin Microbiol Rev.* 2010;23(4):858-883. doi:10.1128/CMR.00007-10
- Abbott NJ, Patabendige AAK, Dolman DEM, Yusof SR, Begley DJ. Structure and function of the blood-brain barrier. *Neurobiol Dis.* 2010;37(1):13-25. doi:10.1016/j.nbd.2009.07.030
- Nau R, Seele J, Djukic M, Eiffert H. Pharmacokinetics and pharmacodynamics of antibiotics in central nervous system infections. *Curr Opin Infect Dis.* 2018;31(1):57-68. doi:10.1097/QCO.0000000000000418
- Galea I. The blood-brain barrier in systemic infection and inflammation. *Cell Mol Immunol.* 2021;18(11):2489-2501. doi:10.1038/s41423-021-00757-x
- Tunkel AR, Hasbun R, Bhimraj A, et al. 2017 Infectious Diseases Society of America's clinical practice guidelines for healthcare-associated ventriculitis and meningitis\*. *Clin Infect Dis.* 2017;64(6):E34-E65. doi:10.1093/cid/ciw861
- Livermore DM. Linezolid in vitro: mechanism and antibacterial spectrum. *J Antimicrob Chemother.* 2003;51(Suppl 2):9-16. doi:10.1093/jac/dkg249
- Tsona A, Metallidis S, Foroglou N, et al. Linezolid penetration into cerebrospinal fluid and brain tissue. *J Chemother.* 2010;22(1):17-19. doi:10.1179/joc.2010.22.1.17
- Luque S, Grau S, Alvarez-Lerma F, et al. Plasma and cerebrospinal fluid concentrations of linezolid in neurosurgical critically ill patients with proven or suspected central nervous system infections. *Int J Antimicrob Agents.* 2014;44(5):409-415. doi:10.1016/j.ijantimicag.2014.07.001
- Barber KE, Smith JR, Raut A, Rybak MJ. Evaluation of tedizolid against *Staphylococcus aureus* and enterococci with reduced susceptibility to vancomycin, daptomycin or linezolid. *J Antimicrob Chemother.* 2016;71(1):152-155. doi:10.1093/jac/dkv302
- Ferry T, Conrad A, Senneville E, et al. Safety of Tedizolid as suppressive antimicrobial therapy for patients with complex implant-associated bone and joint infection due to multidrug-resistant gram-positive pathogens: results from the TediSAT cohort study. *Open Forum Infect Dis.* 2021;8(7):ofab351. doi:10.1093/ofid/ofab351
- Wenzler E, Adeel A, Wu T, et al. Inadequate cerebrospinal fluid concentrations of available salvage agents further impedes the optimal treatment of multidrug-resistant *Enterococcus faecium* meningitis and bacteremia. *Infect Dis Rep.* 2021;13(3):843-854. doi:10.3390/idr13030076
- Gu L, Ma M, Zhang Y, et al. Comparative pharmacokinetics of tedizolid in rat plasma and cerebrospinal fluid. *Regul Toxicol Pharmacol.* 2019;107:104420. doi:10.1016/j.yrtph.2019.104420
- European Medicines Agency. Guideline on bioanalytical method validation. 2011. Accessed September 10, 2024. [www.ema.europa.eu/contact](http://www.ema.europa.eu/contact)
- Slatter JG, Adams LA, Bush EC, et al. Pharmacokinetics, toxicokinetics, distribution, metabolism and excretion of linezolid in mouse, rat and dog. *Xenobiotica.* 2002;32(10):907-924. doi:10.1080/00498250210158249
- Ong V, Flanagan S, Fang E, et al. Absorption, distribution, metabolism, and excretion of the novel antibacterial prodrug tedizolid phosphate. *Drug Metab Dispos.* 2014;42(8):1275-1284. doi:10.1124/dmd.113.056697
- Dabbagh F, Schrotten H, Schwerk C. In vitro models of the blood-cerebrospinal fluid barrier and their applications in the development and research of (neuro)pharmaceuticals. *Pharmaceutics.* 2022;14(8):1729. doi:10.3390/pharmaceutics14081729
- O'brown NM, Pfau SJ, Gu C. Bridging barriers: a comparative look at the blood-brain barrier across organisms. 2018. doi:10.1101/gad.309823
- Peng X, Luo Z, He S, Zhang L, Li Y. Blood-brain barrier disruption by lipopolysaccharide and sepsis-associated encephalopathy. *Front Cell Infect Microbiol.* 2021;11:768108. doi:10.3389/fcimb.2021.768108
- Charlton M, Thompson JP. Pharmacokinetics in sepsis. *BJA Educ.* 2019;19(1):7-13. doi:10.1016/j.bjae.2018.09.006
- Huang L, Wells MC, Zhao Z. A practical perspective on the evaluation of small molecule CNS penetration in drug discovery. *Drug Metab Lett.* 2019;13(2):78-94. doi:10.2174/1872312813666190311125652



21. Morris ME, Rodriguez-Cruz V, Felmlee MA. SLC and ABC transporters: expression, localization, and species differences at the blood-brain and the blood-cerebrospinal fluid barriers. *AAPS J.* 2017;19(5):1317-1331. doi:[10.1208/s12248-017-0110-8](https://doi.org/10.1208/s12248-017-0110-8)
22. Flanagan S, Passarelli J, Lu Q, Fiedler-Kelly J, Ludwig E, Prokocimer P. Tedizolid population pharmacokinetics, exposure response, and target attainment. *Antimicrob Agents Chemother.* 2014;58(11):6462-6470. doi:[10.1128/AAC.03423-14](https://doi.org/10.1128/AAC.03423-14)
23. The European Committee on Antimicrobial Susceptibility Testing. Breakpoint tables EUCAST v14.0. Accessed May 6, 2024. [www.eucast.org](http://www.eucast.org)
24. Constantinescu CS, Farooqi N, O'Brien K, Gran B. Experimental autoimmune encephalomyelitis (EAE) as a model for multiple sclerosis (MS). *Br J Pharmacol.* 2011;164(4):1079-1106. doi:[10.1111/bph.2011.164.issue-4](https://doi.org/10.1111/bph.2011.164.issue-4)
25. Hernández-Rabaza V, Cabrera-Pastor A, Taoro-González L, et al. Hyperammonemia induces glial activation, neuroinflammation and alters neurotransmitter receptors in hippocampus, impairing spatial learning: reversal by sulforaphane. *J Neuroinflammation.* 2016;13(1):41. doi:[10.1186/s12974-016-0505-y](https://doi.org/10.1186/s12974-016-0505-y)

**How to cite this article:** Lahouati M, Oudart M, Alzieu P, Chapouly C, Petitcollin A, Xuereb F. Penetration of linezolid and tedizolid in cerebrospinal fluid of mouse and impact of blood-brain barrier disruption. *Clin Transl Sci.* 2025;18:e70100. doi:[10.1111/cts.70100](https://doi.org/10.1111/cts.70100)

## APPENDIX 1

### Main parameters describing the analytical performances of the methods

|              | Linearity    |              | Intra-day            |               | Inter-day            |               | Sample stability   |                          | Extract stability   |
|--------------|--------------|--------------|----------------------|---------------|----------------------|---------------|--------------------|--------------------------|---------------------|
|              | LLOQ (µg/mL) | ULOQ (µg/mL) | Mean precision (CV%) | Mean bias (%) | Mean precision (CV%) | Mean bias (%) | 3 days at +4°C (%) | 3 freeze-thaw cycles (%) | 7 days at +10°C (%) |
| LNZ (plasma) | 0.1          | 50.0         | 7.30                 | -5.41         | 5.47                 | -8.22         | -4.11              | -9.46                    | -2.26               |
| LNZ (CSF)    | 0.001        | 2.5          | 1.84                 | -3.03         | 6.02                 | 2.76          | 2.49               | -0.04                    | 2.60                |
| TDZ (plasma) | 0.1          | 50.0         | 4.84                 | -2.33         | 11.42                | -7.55         | -6.93              | -12.19                   | -1.95               |
| TDZ (CSF)    | 0.001        | 2.5          | 8.53                 | -6.85         | 2.97                 | -7.04         | -8.44              | -12.16                   | -2.85               |

Abbreviations: CV%, coefficient of Variation; LLOQ, lower limit of quantitation; ULOQ, upper limit of quantitation.

## APPENDIX 2

### Twenty four hours pharmacokinetic of tedizolid without LPS

| Parameters          | Unit    | TDZ (n = 15) |        |
|---------------------|---------|--------------|--------|
|                     |         | Plasma       | CSF    |
| $T_{1/2}$           | h       | 5            | 4.8    |
| $T_{max}$           | h       | 4            | 0.5    |
| $C_{max}$           | ng/mL   | 2761.1       | 187.9  |
| $AUC_{0-24h}$       | ng/mL*h | 32,825.3     | 2356.1 |
| Ratio $AUC_{0-24h}$ | —       | 7.2%         |        |